Crystallization of strongly interacting photons in a nonlinear optical fibre

D. E. CHANG[1], V. GRITSEV[1], G. MORIGI[2], V. VULETIĆ[3], M. D. LUKIN[1] AND E. A. DEMLER[1]*

[1]Department of Physics, Harvard University, Cambridge, Massachusetts 02138, USA

[2]Grup d'Optica, Department de Fisica, Universitat Autonoma de Barcelona, 08193 Bellaterra, Spain

[3]Department of Physics, MIT-Harvard Center for Ultracold Atoms, and Research Laboratory of Electronics, Massachusetts Institute of Technology, Cambridge, Massachusetts 02139, USA

*e-mail: demler@physics.harvard.edu

Published online: 14 September 2008; doi:10.1038/nphys1074

Understanding strongly correlated quantum systems is a central problem in many areas of physics. The collective behaviour of interacting particles gives rise to diverse fundamental phenomena such as confinement in quantum chromodynamics, electron fractionalization in the quantum Hall regime and phase transitions in unconventional superconductors and quantum magnets. Such systems typically involve massive particles, but optical photons can also interact with one another in a nonlinear medium. In practice, however, such interactions are often very weak. Here we describe a technique that enables the creation of a strongly correlated quantum gas of photons using one-dimensional optical systems with tight field confinement and coherent photon trapping techniques. The confinement enables the generation of large, tunable optical nonlinearities via the interaction of photons with a nearby cold atomic gas. In its extreme, we show that a quantum light field can undergo fermionization in such one-dimensional media, which can be probed via standard photon correlation measurements.

Nonlinear effects have long been used to create optical systems with unusual properties[1], and fascinating advances have been made in recent years towards extending these techniques into the few-photon regime[2–4]. Yet the effects of strong correlations manifest themselves most dramatically in many-body systems, often resulting in new states of matter with properties very different from those of the underlying particles. Such phenomena are being actively explored in a variety of condensed-matter systems[5] and with ultracold atoms[6]. One famous example is the Tonks–Girardeau (TG) regime of interacting bosons in one dimension, in which strong interactions lead to an effective 'fermionization' of bosons[7,8]. This unusual regime was recently realized experimentally using ultracold atoms in one-dimensional traps[9,10]. In this article we investigate the feasibility of creating and detecting a TG gas of photons. This system would correspond to nonlinear quantum optics in its extreme, in which individual photons behave as impenetrable particles. In this limit, an optical pulse separates into non-overlapping wave packets of individual photons, and a 'crystal of photons' ensues.

Several papers have recently considered the possibility of phase transitions involving photons using large systems of coupled optical cavities[11–16]. The present study differs from this previous work in several ways. First, although dramatic progress has been achieved in controlling individual atoms and photons in single cavities[2], the complex architecture of coupled cavities proposed in refs 11–16 represents a considerable experimental challenge. In contrast, the approach described here to realize a TG gas of photons involves currently available experimental techniques[17,18]. Second, we show that this state can be created dynamically, without assuming that a thermodynamic equilibrium for many-body photonic states must be achieved. Finally, we describe a technique to read out the properties of the strongly interacting photon gas, and show that these correlations can be detected using standard quantum optical measurements. This potentially enables many new applications and enables us to study even more exotic phenomena involving interacting particles using readily controlled photons with tunable interactions.

STRONGLY INTERACTING PHOTONS IN ONE DIMENSION: THE SYSTEM

Recently, much effort has been directed toward realizing single-mode optical waveguides where the guided photons can be tightly confined to a transverse area A_{eff} near or below the diffraction limit. Such confinement is desirable in part because it enables a large interaction strength between single photons and nearby coupled atoms. Specific systems that have recently been explored include tapered optical fibres[17], hollow-core photonic crystal fibres[18,19], and surface plasmons on conducting nanowires[20,21].

The propagation and interaction of photons in such a medium can be controlled by interfacing them with atoms using quantum optical techniques such as electromagnetically induced transparency (EIT)[4]. In particular, our scheme relies on resonantly enhanced optical nonlinearities with low losses[22] using EIT, and the trapping of stationary pulses of light in the medium using spatially modulated control fields[23] (see Fig. 1a). As will be shown, the dynamical evolution of the photons is governed by an equation that has the form of the nonlinear Schrödinger equation (NLSE), where the signs and strengths of the effective mass and interaction can be controlled using external fields. Under conditions where the nonlinear interaction is large and effectively repulsive, the TG regime of photons can be achieved.

Specifically, we consider the propagation of right- and left-moving quantum fields, characterized by operators $\hat{E}_{\pm}$, inside

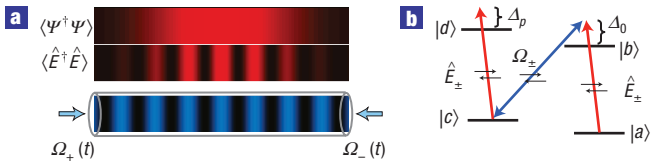

Figure 1 Illustration of fields and atoms comprising the system. a, Schematic diagram of fields inside the waveguide, whose axis of propagation corresponds to the horizontal axis. The control beams $\Omega_{\pm}(t)$ (shown in blue) create a standing wave inside the waveguide, forming a Bragg grating, which traps a quantum optical field inside the medium (intensity $\langle\hat{E}^{\dagger}\hat{E}\rangle$ shown in red). The optical field couples to spin-wave excitations in the medium, resulting in collective polariton excitations, whose density $\langle\Psi^{\dagger}\Psi\rangle$ is also plotted. **b**, Schematic diagram of the four-level atomic configuration and coupling between levels and fields used in our system.

a single-mode waveguide and interacting with cold atoms in the four-level configuration shown in Fig. 1b. The fields $\hat{E}_{\pm}$ couple the ground state $|a\rangle$ (in which the system is initialized) to excited state $|b\rangle$ with a strength given by g, whereas metastable state $|c\rangle$ and $|b\rangle$ are coupled by classical, counter-propagating control fields $\Omega_{\pm}(t)$ (which are also guided). Here, the lambda configuration consisting of states $|a,b,c\rangle$ comprises the typical EIT set-up. In the case where the quantum and classical fields propagate in only one direction, the quantum field can be dynamically and reversibly mapped into a stationary spin-wave excitation by turning the control field $\Omega(t)$ to zero adiabatically. On the other hand, by creating a standing wave formation with the control fields ($\Omega_{+}(t)=\Omega_{-}(t)$), the quantum fields can be effectively stopped although simultaneously maintaining a non-zero photonic component of the excitation (see Fig. 1a)[23]. Intuitively, the standing wave forms reflection gratings that trap the photonic excitations through multiple scattering. The nonlinear response is introduced via an additional state $|d\rangle$ that is coupled to $|c\rangle$ by the quantum fields (for simplicity we also set this coupling strength to be g). When these fields are far off resonance, this coupling results in an a.c. Stark shift of state $|c\rangle$ whose magnitude is proportional to the quantum field intensity[22]. This yields an intensity-dependent refractive index, or nonlinear susceptibility, which in turn influences the evolution of the quantum fields. Although similar schemes for realizing nonlinear optics in atomic media have been previously explored[24], their implementation in tightly confining waveguides is unique because they can constitute a true one-dimensional system, and because the strong transverse localization enables large nonlinear interactions.

THE LIEB–LINIGER MODEL WITH STATIONARY PULSES OF LIGHT

The connections between Maxwell's equations in a one-dimensional nonlinear medium and the Lieb–Liniger model (LLM) describing interacting massive particles have previously been discussed in the literature[25]. However, most of this work has focused on the regime of attractive interactions, the main feature of which is the formation of solitons[25]. This regime of the LLM has few quantum mechanical features and can be mostly described by classical equations of motion. Indeed, typical optical solitons contain of the order of a million photons, and therefore a quasi-classical description is very appropriate[26]. On the other hand, the repulsive case is intrinsically 'quantum mechanical', as we need to keep track of correlations at the level of individual particles. Solutions on the basis of perturbation theory or classical equations break down and we must use non-perturbative approaches such as the Bethe ansatz solution[27–30] or Luttinger liquid formalism[31]. Thus, formation of a TG gas of photons is fundamentally a collective many-body effect.

We now derive an evolution equation for the fields of the system illustrated in Fig. 1. Following the methods of refs 23,24,32, we define dark-state polariton operators $\Psi_{\pm}$ describing the coupled photonic and spin-wave excitations, which in the slow-light limit are given approximately by $\Psi_{\pm}=g\sqrt{2\pi n_z}\hat{E}_{\pm}/\Omega_{\pm}$, where n_z is the density of atoms coupled to the waveguide (the density is assumed to be uniform). We specialize to the case when $\Omega_{\pm}(t)=\Omega(t)$. We further assume that the quantum and control fields vary slowly in time, such that the fast-varying atomic operators can be adiabatically eliminated, whereas the remaining slowly varying operators are solved in the adiabatic limit. Subsequently inserting these solutions into the Maxwell–Bloch equations describing evolution of the quantum fields yields an effective NLSE for the polaritons (see Methods section),

$$i\partial_t\Psi(z,t)=-\frac{1}{2m_{\mathrm{eff}}}\partial_z^2\Psi(z,t)+2\tilde{g}\,\Psi^{\dagger}(z,t)\,\Psi^2(z,t), \qquad (1)$$

where

$$\Psi=\frac{(\Psi_{+}+\Psi_{-})}{2}, \qquad m_{\mathrm{eff}}=-\frac{\Gamma_{1\mathrm{D}}n_z}{4\Delta_0 v_{\mathrm{g}}}, \qquad 2\tilde{g}=\frac{\Gamma_{1\mathrm{D}}v_{\mathrm{g}}}{\Delta_p}. \qquad (2)$$

Here $\Gamma_{1\mathrm{D}}=4\pi g^2/v$ is the spontaneous emission rate of a single atom into the waveguide modes, where v is the velocity of these modes in an empty waveguide, whereas $v_{\mathrm{g}}\approx v\Omega^2/(\pi g^2 n_z)$ is the group velocity of untrapped pulses under EIT conditions. Δ_0 and Δ_p are the one-photon detunings of the fields $\hat{E}_{\pm}$ from the transitions $|a\rangle$–$|b\rangle$ and $|c\rangle$–$|d\rangle$, respectively (see Fig. 1b), and $g\propto 1/\sqrt{A_{\mathrm{eff}}}$ is the single-photon, single-dipole interaction matrix element. In principle, the full dynamics of the field also includes losses and higher-order terms, and the conditions under which they can be ignored are described in the Methods section. We should further note that, despite the standing-wave control field, the evolution of the quantum-field envelope given by equation (1) remains smooth and does not contain features determined by the standing-wave period.

Equation (1) determines the one-dimensional evolution of a quantum field $\Psi(z,t)$ as derived from the Hamiltonian of the Lieb–Liniger model,

$$H=\hbar\int \mathrm{d}z\left[\frac{1}{2m_{\mathrm{eff}}}\partial_z\Psi^{\dagger}(z)\partial_z\Psi(z)+\tilde{g}\,\Psi^{\dagger}(z)\,\Psi^{\dagger}(z)\,\Psi(z)\,\Psi(z)\right]. \qquad (3)$$

The first term on the right describes the kinetic energy of bosons with mass m_{eff}, whereas the second term describes a contact interaction potential. The quantum field $\Psi(z,t)$ satisfies the usual equal-time bosonic commutation relations, $[\Psi(z,t),\Psi^{\dagger}(z',t)]=\delta(z-z')$. The behaviour of this system can be effectively characterized by a single dimensionless parameter

$$\gamma=\frac{m_{\mathrm{eff}}\tilde{g}}{n_{\mathrm{ph}}}=-\frac{\Gamma_{1\mathrm{D}}^2}{8\Delta_0\Delta_p}\frac{n_z}{n_{\mathrm{ph}}}, \qquad (4)$$

which corresponds to the ratio of the interaction and kinetic energies. Here n_{ph} is the linear density of photons at the centre of the pulse. When $\gamma<0$, the interaction with the atoms induces an effective attraction between photons, which is responsible for the formation of bound states (solitons) when a large number of

photons are present, for example. On the other hand, for $\gamma > 0$ the regime of effective repulsion between photons is realized. From equation (2), we find that the regime of repulsion is achieved if exactly one of the detunings Δ_0 or Δ_p is negative. The special limit $\gamma \to \infty$ is called the TG regime[7,8]. In this regime, it can be said that the strongly interacting Bose gas 'fermionizes', in that all of its properties can be derived from those of a non-interacting Fermi gas (and likewise, the bosonic system can be described by effective 'Fermi' momenta and energies)[8]. Finally, we note that $\gamma \propto \Gamma_{1D}^2 \propto A_{eff}^{-2}$, which underscores the importance of tight mode confinement.

One useful feature of this realization of the NLSE is that the parameters m_{eff} and $\tilde{g}$ can be dynamically tuned by varying different parameters of the system. Specifically, both are functions of detuning, and thus γ can be altered either by changing the control field frequencies or by externally manipulating the energies of the atomic levels. As described below, this tunability facilitates the creation of novel photonic states.

PREPARATION AND DETECTION OF STRONGLY CORRELATED PHOTON GAS

The preparation and detection of novel photonic states consists of three basic steps—loading of the pulse, controlled evolution under the NLSE and readout of the final photonic state, each of which we now describe. During the initial loading process, a resonant optical pulse, given by a coherent state, is incident from one direction. It is injected into the waveguide with the copropagating control field (say $\Omega_+(t)$) turned on, whereas the counter-propagating control field $\Omega_-(t)$ is off. This describes the usual situation in EIT, where the input field is mapped into a spatially compressed polariton pulse on entering the medium, which propagates with a variable group velocity $v_g \sim v\Omega_+^2(t)/(g^2 n_z)$. Once the pulse completely enters the medium, $\Omega_+(t)$ is adiabatically turned to zero, reversibly converting the excitations into pure spin-wave form[32]. Under certain conditions this input pulse can be stored with minimal distortion[32], such that all relevant properties (for example field correlations) remain constant during the loading. Following the initial storage, both control fields are then adiabatically switched on, with $\Omega_\pm = \Omega(t)$, during which the pulse becomes trapped and evolves under equation (1). The parameters m_{eff} and $\tilde{g}$ can be changed in time during the evolution to reach the final state of interest. Here, we propose to create a TG gas of polaritons through adiabatic transformation by varying these parameters such that $\gamma(t)$ adiabatically increases from zero to a large value. During this process the initial coherent state, which is an eigenstate of the initial non-interacting Hamiltonian, remains an eigenstate of the instantaneous Hamiltonian, so that it finally reaches the TG regime. This method differs from the proposals of refs 11–16, where assumptions of either thermodynamic equilibrium or numerical simulations of few-photon dynamics are used to infer the existence of strongly correlated systems. Once this state has been achieved, the pulse is released by turning one of the control fields (say Ω_-) off, thereby enabling the pulse to propagate undistorted until it exits the waveguide[23]. During this stage, any spatial correlations that formed in the polaritons while evolving under the NLSE are directly mapped into temporal correlations (at a common point in space) of purely outgoing photons, which can be measured using standard quantum optical techniques. An appealing feature of this approach is that the pulse velocity as it exits the waveguide is determined by the control field. In particular, the timing and bandwidth of the outgoing pulse can be specified without affecting the underlying quantum correlations, which enables us to efficiently probe the field properties after exiting.

A characteristic signature of a strongly interacting gas is the appearance of Friedel oscillations[33] in the normalized second-order correlation function, $g^{(2)}(z,z') = \langle I(z)I(z')\rangle/(\langle I(z)\rangle\langle I(z')\rangle)$, where $I(z) = \Psi^\dagger(z)\Psi(z)$ is the stationary pulse intensity before release. Specifically, if a photonic state close to the LLM ground state is created, $g^{(2)}(z,z')$ contains an oscillating part that behaves as $\sim \cos(2k_F(z-z'))$ (see the Methods section). Here $k_F = \pi n_{ph}$ is the 'Fermi momentum' in the TG limit. In the TG limit, the ground-state correlation function takes on a simple form[34],

$$g^{(2)}_{TG}(z,z') = 1 - \left(\frac{\sin k_F(z-z')}{k_F(z-z')}\right)^2 .$$

The $2k_F$ oscillations are a direct manifestation of 'fermionization' of bosons. The Friedel oscillations represent more than simple antibunching in that they indicate real crystal correlations. In particular, we cannot predict the position of an individual photon, but, knowing the position of one, other photons are likely to follow at well-defined distances determined by the average photon density. These correlations are predicted to decay relatively slowly in space. We emphasize that the oscillation period depends only on the density of photons n_{ph} inside the medium and not on the standing-wave period ($\sim\lambda/2$) of the control fields. These two length scales can be dramatically different and thus the observation of Friedel oscillations indicates a true 'self-organization' process.

The usual definition of the TG regime of the LLM is given with respect to the equilibrium state. However, in our system the field evolution under the NLSE inherently involves non-equilibrium quantum dynamics. Therefore we must specify the conditions under which we can obtain a strongly interacting state of photons that remains close to the LLM ground state and shows its characteristic features, such as Friedel oscillations. To be concrete, we consider the evolution of a pulse under equation (1) where the effective mass m_{eff} is constant in time, whereas the interaction strength $\tilde{g}(t)$ increases exponentially. Following equation (4), we write the time-dependent interaction parameter in the form $\gamma = \gamma_0 e^{\beta\omega_F t}$, where β is a dimensionless parameter characterizing the rate of increase, and $\omega_F \sim n_{ph}^2/m_{eff}$ corresponds to the 'Fermi energy' at the centre of the pulse before expansion. We assume that $\gamma_0 \ll 1$, thus yielding an initial system of non-interacting photons, and interactions are gradually switched on to reach the regime $\gamma \gg 1$. Here we will not discuss the effect

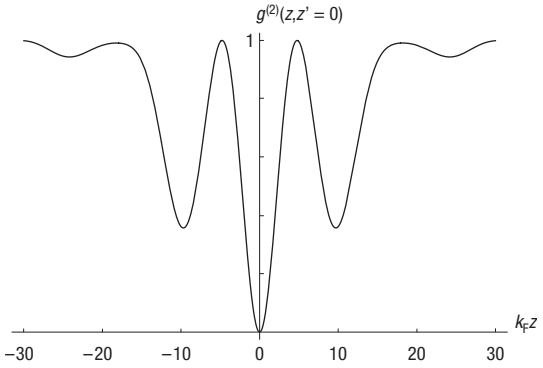

Figure 2 Density–density correlation function $g^{(2)}(z, z' = 0)$ for an expanding TG gas of photons with initial density profile $n_{ph}(z) = n_0(1 - z^2/z_0^2)^{1/2}$. This expansion is equivalent to the problem of a TG gas released from an initial parabolic confining potential. $z' = 0$ denotes the centre of the pulse, and distances are indicated in units of k_F^{-1}. The density–density correlation function shown here is for a system of $N_{ph} = 10$ photons, $z_0 \approx 5k_F^{-1}$ and time $t = 10\omega_F^{-1}$ following the initial release.

of a time-dependent mass, although it can be included using a similar analysis.

The non-equilibrium dynamics of the LLM has previously been studied in the context of ultracold atoms and has focused on either a changing interaction strength in a system with uniform, constant density[35,36], or the expansion of particles in a system with constant interaction[37,38]. In our system both processes take place, but in the experimentally relevant regime of large photon number there is a separation of timescales that simplifies the analysis.

Specifically, we consider an initial pulse containing $N_{\rm ph} \sim n_{\rm ph} z_0$ photons with spatial extent z_0 at $t = 0$. Our discussion applies for a general pulse shape and thus we need not specify it. There are three distinct regimes in the pulse evolution: (1) Interactions are weak and the photons expand freely owing to dispersion. (2) Interactions begin to dominate over the kinetic energy. However, the system is still in the weakly interacting regime with $\gamma < 1$, resulting in hydrodynamic expansion[39,40]. (3) The system reaches the strongly interacting regime with $\gamma > 1$, and the expansion resembles that of fermionized bosons[37,38]. A simple analysis (see the Methods section) shows that by the time the system reaches regime (3) the relative change in the photon density at the centre of the pulse is only of the order of $1/\beta^2 N_{\rm ph}^2$. Hence for $\beta N_{\rm ph} \gg 1$ we can assume that the turning on of interactions occurs at constant density, and any subsequent expansion takes place in the TG regime.

We now consider the effect of non-adiabaticity on correlation functions such as $g^{(2)}(z, z')$. By analogy with ultracold atoms, we introduce an effective chemical potential, which in regimes (1) and (2) is given by $\mu(t) \approx \tilde{g}(t) n_{\rm ph}$ (ref. 6). We can approximately separate the turning on of interactions into two stages, which both take place during regime (1) or (2). In the first stage, $\dot{\mu} > \mu^2$ and the adiabatic transformation is inefficient. In the second stage, $\dot{\mu} < \mu^2$ and the evolution is essentially adiabatic. At the time $t_{\rm adiab}$ separating the two regimes, the interaction parameter is given by $\gamma(t_{\rm adiab}) \sim \beta$. The first stage can be thought of as an instantaneous projection of the wavefunction, which gives rise to a finite density of excitations characterized by an effective healing length $\xi_{\rm neq} \sim (\mu(t) m_{\rm eff})^{-1/2}$ at time $t_{\rm adiab}$. During the second stage, the number of excitations does not change. Hence, the finite rate of change of the interaction strength leads to a finite correlation length in our system, $\xi_{\rm neq} \sim \beta^{-1/2} n_{\rm ph}^{-1}$. At distances shorter than $\xi_{\rm neq}$ all correlation functions are essentially the same as in the ground state, whereas for distances longer than $\xi_{\rm neq}$ correlation functions rapidly decay. To observe Friedel oscillations over length scales of the order of the inter-photon distance, for example, requires that $\beta \lesssim 1$. The argument presented above can be turned into a quantitative calculation for the correlation functions following a time-dependent change in the interaction strength[36]. This analysis uses bosonization to treat the LLM and the conclusions agree with the qualitative picture presented here.

At the end of regime (2) we have a system of 'fermionized' hard-core photons that should show Friedel oscillations. In regime (3), the pulse of hard-core photons expands, but such spreading does not lead to suppression of the Friedel oscillations[37,38]. The problem of expansion of hard-core photons starting from a general pulse shape has to be analysed numerically. However, an explicit analytic solution is available for a parabolic pulse shape. Under realistic conditions, this solution (see Methods section) yields the correlation function shown in Fig. 2.

During the evolution we must also consider the effects of incoherent photon scattering or absorption, which set a maximum evolution time $t_{\rm max}$ and interaction parameter $\gamma_{\rm max}$ that can be achieved before a substantial fraction of the initial pulse is lost. The number of photons absorbed during the evolution has been calculated in Supplementary Information, and requiring that this quantity be small yields the following limit on the maximum achievable interaction parameter:

$$\gamma_{\rm max} \sim \min\left(\gamma_0 \exp\left(\frac{\beta|\Delta_0|}{\Gamma}\right), \eta\beta \frac{\Gamma}{|\Delta_0|}\frac{\rm OD}{N_{\rm ph}}\right).$$

Here Γ is the total spontaneous emission rate of states $|b\rangle$ and $|d\rangle$ (assumed to be equal for simplicity), which includes the emission rate into the waveguide modes ($\Gamma_{\rm 1D}$) as well as non-guided modes (for example, into free space). We have also defined a 'single-atom cooperativity' $\eta = \Gamma_{\rm 1D}/\Gamma$ ($\eta \leq 1$), which describes the efficiency of coupling to the waveguide, and defined the optical depth of the medium, ${\rm OD} = \eta z_0 n_z$. We note that $\gamma_{\rm max}$ improves with increasing optical depth or cooperativity of the system, and can be optimized by adjusting the detuning $|\Delta_0|$. The optimal values of $\gamma_{\rm max}$, as functions of OD and η, are plotted in Fig. 3, for parameters $\beta = 1$, $\gamma_0 = 0.1$ and $N_{\rm ph} = 10$. We see that with realistic values of OD $\sim$ 2,000 and $\eta \sim 0.2$, for example, a value of $\gamma_{\rm max} \sim 10$ is achievable. Although photon losses limit the maximum evolution time, somewhat surprisingly the nonlinear losses may also help in bringing the system closer to the LLM ground state. Specifically, these losses predominantly remove states in which two photons are close to each other, which correspond to high-energy states of the LLM. Deep in the TG regime we can estimate the rate at which high-energy states are lost, $t_{\rm en}^{-1} \approx (\Gamma/\Delta_p)\tilde{g} n_{\rm ph}$. On the other hand, the overall photon loss rate is $t_{\rm los}^{-1} \approx (\Gamma/\Delta_p)\omega_{\rm F}$. Thus $t_{\rm en}/t_{\rm los} \approx \gamma^{-1}$ and for large γ there is a sufficient time window for the high-energy states to decay before too many photons are lost.

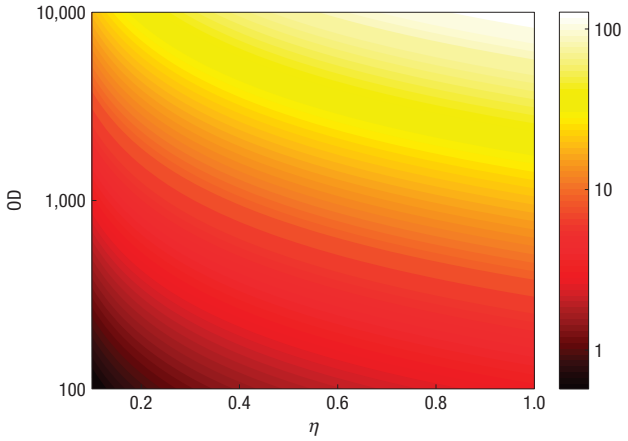

Figure 3 Maximum interaction parameter $\gamma_{\rm max}$ as functions of optical depth and single-atom cooperativity, optimized over the detuning Δ_0. $\gamma_{\rm max}$ is plotted for fixed values of $\beta = 1$, $\gamma_0 = 0.1$, and $N_{\rm ph} = 10$. It is evident that the TG regime for photons can be approached by increasing either the cooperativity or optical depth.

OUTLOOK

The above analysis indicates that strongly correlated states of photons can be controllably prepared and observed using one-dimensional waveguides and quantum optical techniques such as EIT, which make the system widely tunable. Such states should find numerous applications. A crystal of photons is a promising candidate for applications in metrology and quantum information, for example. In particular, these states feature strongly suppressed photon-number fluctuations within a given detection interval, and might be useful as an input for sub-shot-noise interferometers[41,42], or in extension to schemes for quantum

computing[43] or quantum cryptography[44] that rely on single photons. Another exciting direction is quantum simulation of matter Hamiltonians using optical systems. Thus far, we have considered photons with only one polarization, yet including photons of different polarizations should be equivalent to adding a spin degree of freedom to effective matter Hamiltonians. This opens up exciting prospects for exploring spin–charge separation[45] and modelling exotic spin systems (similar to those emerging from multicomponent Bose–Hubbard models[46]). The level structure of the atoms comprising the medium can also vary considerably, which might be used to study strongly correlated systems with non-abelian symmetry, similar to the ones realized in multichannel Kondo models and quantum chromodynamics. Possible phase transitions in these models are difficult, if possible at all, to realize in matter systems. Furthermore, it would be interesting to consider a situation where interactions between the cold atoms create non-trivial correlations[47] and their effect on the resulting photonic states. Therefore, using light to simulate matter Hamiltonians could give a new meaning to the old idea of particle–wave duality.

METHODS

DERIVATION OF THE NONLINEAR SCHRÖDINGER EQUATION FOR PHOTONS

The Hamiltonian corresponding to the system described in Fig. 1 is given in a rotating frame by

$$\begin{aligned} H &= -\hbar n_z \int \mathrm{d}z[\Delta_0\sigma_{bb}+\Delta_p\sigma_{dd} \\ &\quad + g\sqrt{2\pi}((\sigma_{ba}+\sigma_{dc})(\hat{E}_+\mathrm{e}^{ik_0z}+\hat{E}_-\mathrm{e}^{-ik_0z})+\mathrm{h.c.}) \\ &\quad + ((\Omega_+(t)\mathrm{e}^{ik_cz}+\Omega_-(t)\mathrm{e}^{-ik_cz})\sigma_{bc}+\mathrm{h.c.})], \end{aligned}$$

where $\hat{E}_\pm \equiv \hat{E}_\pm(z,t)$ are slowly varying operators describing the quantum fields, $\sigma_{ij} \equiv \sigma_{ij}(z,t)$ are collective, continuous operators describing the average of $|i\rangle\langle j|$ over atoms in a small but macroscopic region around z, and k_0 and k_c are the wavevectors corresponding to the central frequencies of the quantum and control fields, respectively. For simplicity, we have assumed equal transition matrix elements $g_{ba}=g_{dc}=g$ between the quantum fields $\hat{E}_\pm$ and the transitions $|a\rangle$–$|b\rangle$ and $|c\rangle$–$|d\rangle$, where $g_{ij} \sim \langle i|d|j\rangle\sqrt{\omega_{ij}/\hbar\epsilon_0 A_{\mathrm{eff}}}$ and $\langle i|d|j\rangle$ is the dipole matrix element. Defining slowly varying operators $\sigma_{ab}=\sigma_{ab,+}\mathrm{e}^{ik_0z}+\sigma_{ab,-}\mathrm{e}^{-ik_0z}$ and $\sigma_{cd}=\sigma_{cd,+}\mathrm{e}^{ik_0z}+\sigma_{cd,-}\mathrm{e}^{-ik_0z}$, the Maxwell–Bloch equations describing the evolution of the fields under H are given by

$$\left(\frac{1}{v}\frac{\partial}{\partial t}\pm\frac{\partial}{\partial z}\right)\hat{E}_\pm(z,t)=\frac{\sqrt{2\pi}ign_z}{v}\left(\sigma_{ab,\pm}(z,t)+\sigma_{cd,\pm}(z,t)\right), \qquad (5)$$

whereas the usual Langevin–Bloch equations describing evolution of σ_{ij} can be derived following the methods of refs 23,24,32. Following these references, we define polariton operators $\Psi_\pm$ to describe the collective excitations of field and spin-wave coherence σ_{ac} that result from coupling with the control fields, which in the relevant limit where the excitations are mostly in spin-wave form are given by $\Psi_\pm = g\sqrt{2\pi n_z}\hat{E}_\pm/\Omega_\pm$. To proceed further, we adiabatically eliminate the Langevin–Bloch equations for the fast-decaying atomic operators (for example σ_{ab} and σ_{cd}), and slowly varying operators are solved in terms of $\Psi_\pm$, discarding higher time derivatives in the slowly varying limit. Plugging these results back into equation (5), and specializing to the case where $\Omega_\pm(t)=\Omega$, we obtain evolution equations for the polaritons alone,

$$\frac{1}{v}\partial_t\Psi+\partial_z A=-\frac{1}{v_g}\partial_t\Psi-\frac{2\pi ig^2}{v(2\Delta_p+i\Gamma)}\left(2\Psi^\dagger\Psi+A^\dagger A\right)\Psi+\mathrm{noise}, \qquad (6)$$

$$\frac{1}{v}\partial_t A+\partial_z\Psi=-\frac{4\pi g^2n_z}{v(\Gamma-2i\Delta_0)}A-\frac{2\pi ig^2}{v(2\Delta_p+i\Gamma)}\Psi^\dagger\Psi A+\mathrm{noise}.$$

Here we have defined the symmetric and antisymmetric combinations $\Psi=(\Psi_+ + \Psi_-)/2$ and $A=(\Psi_+ - \Psi_-)/2$, and a group velocity $v_g \approx v\Omega^2/(\pi g^2 n_z)$ under which the pulses would propagate were they not trapped. The total spontaneous emission rates Γ (which include decay into channels other than the guided fibre modes) from states $|b\rangle, |d\rangle$ are assumed to be identical for simplicity. We note that there are also noise operators, which are associated with the dissipative terms in the equations above. Because we are primarily interested in the regime where losses are not significant, the specific form of these operators is not important here. With sufficient optical depth, A can be adiabatically eliminated, $A \approx (2i\Delta_0-\Gamma)v(\partial_z\Psi)/(4\pi g^2 n_z)$, where we have assumed that the nonlinear contribution $\sim\Psi^\dagger\Psi A$ is small. Physically, this result corresponds to a pulse-matching phenomenon[48] between the quantum and control fields, whereby any imbalance between Ψ_+ and Ψ_- rapidly goes to zero. Substituting the expression for A back into equation (6), and considering the relevant case where $v_g \ll v$ yields the NLSE with complex effective mass and two-body interaction strength,

$$i\partial_t\Psi=\frac{(2\Delta_0+i\Gamma)v_g v}{4\pi g^2 n_z}\partial_z^2\Psi+\frac{4\pi g^2 v_g}{v(\Delta_p+i\Gamma/2)}\Psi^\dagger\Psi^2+\mathrm{noise}. \qquad (7)$$

Identifying $\Gamma_{1D}=4\pi g^2/v$ and ignoring the loss terms reproduces the ideal NLSE given in equation (1).

We now consider the limits under which equation (1) well approximates the complete dynamics of the field. First, the a.c. Stark shift of $|c\rangle$ due to the nonlinear interaction must fit within the frequency range where EIT is efficient (that is, within the transparency window), which is conservatively satisfied when $n_{ph}/n_z \ll |\Delta_p|/|\Gamma-2i\Delta_0|$. In addition, requiring that higher-order derivatives of the field be negligible compared with those appearing in equation (1) places a restriction on the maximum wavevector k_{max} of the spin-wave excitation. In the TG regime, for example, $k_{max} \sim n_{ph}$ and we consequently find that $n_{ph}/n_z \ll \Gamma_{1D}/|2\Delta_0+i\Gamma|$. Finally, as discussed further in Supplementary Information, we must also ensure that the loss terms in equation (7) do not cause the dissipation of too many photons, which sets a maximum allowed evolution time t_{max} for the system.

DENSITY–DENSITY CORRELATIONS IN A ONE-DIMENSIONAL SYSTEM OF BOSONS

Evaluation of the density–density correlation function in the ground state is challenging even though the Hamiltonian in equation (3) is exactly solvable. However, in the regime of interest where γ is large we can obtain an analytic expression[28] (we assume that translational invariance is present and therefore $g^{(2)}(z_1,t_1;z_2,t_2)=g^{(2)}(z_1-z_2=\Delta z,t_1-t_2=\Delta t)$),

$$\begin{aligned} g^{(2)}(\Delta z,\Delta t) &= 1+\frac{K}{4\pi^2 n_{ph}^2}\int_{|q_1|>\pi n_{ph}}\mathrm{d}q_1\int_{|q_2|<\pi n_{ph}}\mathrm{d}q_2\mathrm{e}^{it(q_1^2-q_2^2)} \\ &\quad\times\cos[(q_1-q_2)z\sqrt{K}] \\ &\quad\times\left[1+\frac{q_1-q_2}{\pi\tilde{g}}\int_{-\pi n_{ph}}^{\pi n_{ph}}\mathrm{d}q_3\left(\frac{1}{q_3-q_1}-\frac{1}{q_3-q_2}\right)\right], \end{aligned}$$

where $K=1+4/\gamma$. Note that $g^{(2)}$ decays as t^{-1} for a range of $t>0$.

For arbitrary interaction strength we can use the exact solution to numerically evaluate $g^{(2)}$ (refs 28–30). On the other hand this numerical solution[29,30] as well as a number of other arguments[31,49] suggests that an effective description of a one-dimensional gas of bosons, the Luttinger liquid theory, provides very good long-distance, long-time behaviour. Using this theory, we can demonstrate that the density–density correlation function in the ground state shows a power-law decay of correlations and $2k_F$ Friedel oscillations,

$$\begin{aligned} g^{(2)}(\Delta z,\Delta t) &= 1+\frac{K}{2\pi^2 n_{ph}^2}\frac{(\Delta z)^2-(v_g\Delta t)^2}{[(\Delta z)^2+(v_g\Delta t)^2]^2} \\ &\quad+\frac{B\cos(2k_F\Delta z)}{n_{ph}^2|\Delta z+iv_g\Delta t|^{2K}}, \end{aligned}$$

where B is a non-universal constant. The interaction parameter K, or Luttinger parameter[31,49], can be numerically extracted from the exact solution. In the limit of strong interactions, $K=1+4/\gamma$ and tends to unity in the TG regime. Here $k_F=\pi n_{ph}$ is an emergent Fermi momentum.

In the case of sudden switch-on of the interaction, we can use the completeness of the Bethe Ansatz wavefunction basis and expand the initial state over this basis. As the matrix elements of the density operator in the Bethe states are known[50], computation of the density–density correlation function starting from an arbitrary initial state can in principle be carried out.

EXPANSION OF THE PULSE

We consider the expansion of the optical pulse during stages (1) and (2) introduced in the section 'Preparation and detection of strongly correlated photon gas'. In regime (1), the interaction energy of particles can be ignored in comparison with the kinetic energy as long as $\tilde{g}(t)n_{\rm ph}$ is smaller than the kinetic energy $1/m_{\rm eff}z_0^2$. The time t_1 at which these energies become comparable satisfies $t \propto -\log(N_{\rm ph}^2\gamma_0)$, and thus if we choose parameters such that $N_{\rm ph}^2\gamma_0 > 1$ free expansion can be ignored (for large photon number we can simultaneously satisfy $\gamma_0 \ll 1$ such that the system is initially non-interacting). Regime (2), which is valid until $\gamma(t=t_{\rm c})=1$, can be analysed using the usual hydrodynamic equations (see, for example, refs 39,40). From the equation of motion for the flow velocity, we find $\dot{v}(t) \sim (n_{\rm ph}/m_{\rm eff}z_0)g(t)$, and from the conservation of particle number, $\dot{n}_{\rm ph}(t) \sim (n_{\rm ph}/z_0)v(t)$. Assuming that the change in density at the centre of the pulse is small, these equations can be integrated to yield a relative change of density $\Delta n_{\rm ph}/n_{\rm ph} \sim 1/\beta^2 N_{\rm ph}^2$.

Next we consider the expansion in the strongly interacting regime. Recent work[37,38] has demonstrated that spreading of a pulse of hard-core bosons enhances the 'fermionic' character of the wavefunction[37]. Although generally this problem requires numerical simulations, the solution turns out to be extremely simple for an initial pulse density of the form $n_{\rm ph}(z) = n_0(1-z^2/z_0^2)^{1/2}$, which corresponds to hard-core bosons released from a parabolic potential[38]. In this case the structure of the density correlations is preserved and there is only a rescaling of length scales[38]. An explicit calculation of $g^{(2)}$ for this system is shown in Fig. 2. Another signature of fermionization of an expanding pulse of hard-core bosons can be observed in the momentum distribution function $n(k)$ (density at wavevector k), corresponding to the Fourier transform of the first-order correlation function $g^{(1)}(z,z') = \langle\psi(z)\psi^{\dagger}(z')\rangle$. After sufficiently long expansion it approaches a Fermi distribution[37,38]. The qualitative features of our results remain valid for various initial pulse shapes, although numerical analysis is needed to obtain precise answers.

Received 7 December 2007; accepted 14 August 2008; published 14 September 2008.

References

1. Boyd, R. W. *Nonlinear Optics* (Academic, New York, 1992).
2. Haroche, S. & Raimond, J. M. *Exploring the Quantum: Atoms, Cavities and Photons* (Oxford Univ. Press, New York, 2006).
3. Birnbaum, K. M. *et al.* Photon blockade in an optical cavity with one trapped atom. *Nature* **436**, 87–90 (2005).
4. Fleischhauer, M., Imamoglu, A. & Marangos, J. P. Electromagnetically induced transparency: Optics in coherent media. *Rev. Mod. Phys.* **77**, 633–675 (2005).
5. Auslaender, O. M. *et al.* Spin–charge separation and localization in one dimension. *Science* **308**, 88–92 (2005).
6. Bloch, I., Dalibard, J. & Zwerger, W. Many-body physics with ultracold gases. *Rev. Mod. Phys.* **80**, 885–964 (2008).
7. Tonks, L. The complete equation of state of one, two and three-dimensional gases of hard elastic spheres. *Phys. Rev.* **50**, 955–963 (1936).
8. Girardeau, M. Relationship between systems of impenetrable bosons and fermions in one dimension. *J. Math. Phys.* **1**, 516–523 (1960).
9. Kinoshita, T., Wenger, T. & Weiss, D. S. Observation of a one-dimensional Tonks–Girardeau gas. *Science* **305**, 1125–1128 (2004).
10. Paredes, B. *et al.* Tonks–Girardeau gas of ultracold atoms in an optical lattice. *Nature* **429**, 277–281 (2004).
11. Hartmann, M. J., Brandão, F. G. S. L. & Plenio, M. B. Strongly interacting polaritons in coupled arrays of cavities. *Nature Phys.* **2**, 849–855 (2006).
12. Greentree, A. D., Tahan, C., Cole, J. H. & Hollenberg, L. C. L. Quantum phase transitions of light. *Nature Phys.* **2**, 856–861 (2006).
13. Angelakis, D. G., Santos, M. F. & Bose, S. Photon-blockade-induced Mott transitions and XY spin models in coupled cavity arrays. *Phys. Rev. A* **76**, 031805(R) (2007).
14. Na, N., Utsunomiya, S., Tian, L. & Yamamoto, Y. Strongly correlated photons in a two-dimensional array of photonic crystal microcavities. *Phys. Rev. A* **77**, 031803(R) (2008).
15. Hartmann, M. J. & Plenio, M. B. Strong photon nonlinearities and photonic Mott insulators. *Phys. Rev. Lett.* **99**, 103601 (2007).
16. Rossini, D. & Fazio, R. Mott-insulating and glassy phases of polaritons in 1D arrays of coupled cavities. *Phys. Rev. Lett.* **99**, 186401 (2007).
17. Nayak, K. P. *et al.* Optical nanofiber as an efficient tool for manipulating and probing atomic fluorescence. *Opt. Express* **15**, 5431–5438 (2007).
18. Ghosh, S., Sharping, J. E., Ouzounov, D. G. & Gaeta, A. L. Resonant optical interactions with molecules confined in photonic band-gap fibers. *Phys. Rev. Lett.* **94**, 093902 (2005).
19. Knight, J. C. Photonic crystal fibers. *Nature* **424**, 847–851 (2003).
20. Chang, D. E., Sørensen, A. S., Hemmer, P. R. & Lukin, M. D. Quantum optics with surface plasmons. *Phys. Rev. Lett.* **97**, 053002 (2006).
21. Akimov, A. V. *et al.* Generation of single optical plasmons in metallic nanowires coupled to quantum dots. *Nature* **450**, 402–406 (2007).
22. Schmidt, H. & Imamoglu, A. Giant Kerr nonlinearities obtained by electromagnetically induced transparency. *Opt. Lett.* **21**, 1936–1938 (1996).
23. Bajcsy, M., Zibrov, A. S. & Lukin, M. D. Stationary pulses of light in an atomic medium. *Nature* **426**, 638–641 (2003).
24. Bajcsy, M, Andre, A., Zibrov, A. S. & Lukin, M. D. Nonlinear optics with stationary pulses of light. *Phys. Rev. Lett.* **94**, 063902 (2005).
25. Lai, Y. & Haus, H. A. Quantum theory of solitons in optical fibers. II. Exact solution. *Phys. Rev. A* **40**, 854–866 (1989).
26. Mazets, I. E. & Kurizki, G. How different are multiatom quantum solitons from mean-field solitons? *Europhys. Lett.* **76**, 196–202 (2006).
27. Lieb, E. H. & Liniger, W. Exact analysis of an interacting Bose gas. I. The general solution and the ground state. *Phys. Rev.* **130**, 1605–1616 (1963).
28. Korepin, V. E., Bogoliubov, N. M. & Izergin, A. G. *Quantum Inverse Scattering Method and Correlation Functions* (Cambridge Univ. Press, Cambridge, 1993).
29. Caux, J.-S. & Calabrese, P. Dynamical density–density correlations in the one-dimensional Bose gas. *Phys. Rev. A* **74**, 031605 (2006).
30. Caux, J.-S., Calabrese, P. & Slavnov, N. A. One-particle dynamical correlations in the one-dimensional Bose gas. *J. Stat. Mech.* P01008 (2007).
31. Haldane, F. D. M. Effective harmonic-fluid approach to low-energy properties of one-dimensional quantum fluids. *Phys. Rev. Lett.* **47**, 1840–1843 (1981); erratum **48**, 569 (1982).
32. Fleischhauer, M. & Lukin, M. D. Dark-state polaritons in electromagnetically induced transparency. *Phys. Rev. Lett.* **84**, 5094–5097 (2000).
33. Friedel, J. Metallic alloys. *Nuovo Cimento* **7**, 287–311 (1958).
34. Lenard, A. One-dimensional impenetrable bosons in thermal equilibrium. *J. Math. Phys.* **7**, 1268–1272 (1966).
35. Cazalilla, M. A. Effect of suddenly turning on interactions in the Luttinger model. *Phys. Rev. Lett.* **97**, 156403 (2006).
36. Polkovnikov, A. & Gritsev, V. Breakdown of the adiabatic limit in low-dimensional gapless systems. *Nature Phys.* **4**, 477–481 (2008).
37. Rigol, M. & Muramatsu, A. Free expansion of impenetrable bosons on one-dimensional optical lattices. *Mod. Phys. Lett. B* **19**, 861–881 (2005).
38. Minguzzi, A. & Gangardt, D. M. Exact coherent states of a harmonically confined Tonks–Girardeau gas. *Phys. Rev. Lett.* **94**, 240404 (2005).
39. Castin, Y. & Dum, R. Bose–Einstein condensates in time dependent traps. *Phys. Rev. Lett.* **77**, 5315–5319 (1996).
40. Kagan, Yu., Surkov, E. L. & Shlyapnikov, G. V. Evolution of a Bose-condensed gas under variations of the confining potential. *Phys. Rev. A* **54**, R1753–R1756 (1996).
41. Dowling, J. P. Correlated input-port, matter-wave interferometer: Quantum-noise limits to the atom-laser gyroscope. *Phys. Rev. A* **57**, 4736–4746 (1998).
42. Bouyer, P. & Kasevich, M. A. Heisenberg-limited spectroscopy with degenerate Bose–Einstein gases. *Phys. Rev. A* **56**, R1083–R1086 (2002).
43. Kok, P. *et al.* Linear optical quantum computing with photonic qubits. *Rev. Mod. Phys.* **79**, 135–174 (2007).
44. Gisin, N., Ribordy, G., Tittel, W. & Zbinden, H. Quantum cryptography. *Rev. Mod. Phys.* **74**, 145–195 (2002).
45. Schulz, H. J. in *Mesoscopic Quantum Physics, Proc. Les Houches Summer School LXI* (eds Akkermans, E., Montambaux, G., Pichard, J. & Zinn-Justin, J.) 533–603 (Elsevier, Amsterdam, 1995).
46. Hartmann, M. J., Brandão, F. G. S. L. & Plenio, M. B. A polaritonic two-component Bose–Hubbard model. *New J. Phys.* **10**, 033011 (2008).
47. Mašalas, M. & Fleischhauer, M. Scattering of dark-state polaritons in optical lattices and quantum phase gates for photons. *Phys. Rev. A* **69**, 061801(R) (2004).
48. Harris, S. E. Electromagnetically induced transparency with matched pulses. *Phys. Rev. Lett.* **70**, 552–555 (1993).
49. Giamarchi, T. *Quantum Physics in One Dimension* (Oxford Univ. Press, New York, 2004).
50. Slavnov, N. A. Nonequal-time current correlation function in a one-dimensional Bose gas. *Theor. Math. Phys.* **82**, 273–282 (1990).

Supplementary Information accompanies the paper at www.nature.com/naturephysics.

Acknowledgements

We gratefully acknowledge support from the NSF, Harvard–MIT CUA, DARPA, Air Force and Packard Foundation.

Author information

Reprints and permissions information is available online at http://npg.nature.com/reprintsandpermissions.
Correspondence and requests for materials should be addressed to E.A.D.